Single well or double well: First-principles study of 8*H* and 3*C* inclusions in the 4*H* SiC polytype

Mao-Sheng Miao
Materials Research Laboratory, University of California Santa Barbara, California 93106, USA and
Beijing Computational Science Research Center, Beijing 100084, People's Republic of China

Walter R. L. Lambrecht
Department of Physics, Case Western Reserve University, 10900 Euclid Ave., Cleveland, Ohio 44106-7079, USA
(Received 19 April 2012; published 29 May 2012)

Using first-principles calculations with a hybrid functional, we examined several fundamental issues for heterojunction structures formed by the same material but in different polytypes including the precise location of the boundary and the polarization. Particularly, we demonstrate that the inclusion of 8*H* in 4*H* SiC generates a single quantum well (QW) structure, rather than a double well consisting of two 3*C* regions separated by a single hexagonal layer barrier. The level of the QW states for 8*H* and 3*C* inclusions are calculated to be 0.42 and 0.68 eV, respectively, below the conduction band minimum of 4*H* SiC, in good agreement with the experiments.

DOI: 10.1103/PhysRevB.85.205318 PACS number(s): 61.72.Nn, 73.21.Cd, 73.40.Lq

I. INTRODUCTION

The most distinctive property of SiC is its ability to form many different polytypes,[1] among which the most frequently studied ones are 3*C*, 4*H*, and 6*H*. The structural variations are accompanied by a large variation in the electronic structures and properties, including the band gaps and the effective electron masses.[2,3] Since the band gap can vary from 3.33 eV for 2*H* to 2.42 eV for 3*C* materials, growing different SiC polytypes in adjacent layers may form quantum wells (QWs) or superlattices.[4–6] The discovery of the frequent occurrence of 3*C* inclusions in 4*H* SiC caused by double stacking fault growth for heavily *n*-doped samples under annealing[7–9] shows a possibility of fabricating QW structures[10–12] based on different SiC polytypes.

Recently the inclusion of the 8*H* polytype in 4*H* SiC was found in as-grown samples,[13,14] which adds an interesting new member to the heteropolytype QWs. The major difference between the 8*H* inclusion and the 3*C* inclusion is the present of one extra hexagonal layer in the middle of the cubic layers. An important issue then arises: Will the system behave like a single QW or like two adjacent wells separated by a single hexagonal layer [Fig. 1]? A recent work suggests the latter scenario by comparing the photoluminescence spectra and QW simulations based on the effective mass approximation.[15] However, it is not entirely clear whether this approximation is valid for an ultrathin QW structure.

Another fundamental issue is general to all heterojunctions formed by polytypes: Where is the boundary between different regions? For example in the 4*H*/3*C*/4*H* QW, the 4*H* region has alternating cubic and hexagonal layers, *hchchchc*$\cdots$, whereas the 3*C* region only consists of cubic layers, *ccccc*$\cdots$. Should the 3*C* region in a 4*H*/3*C*/4*H* QW start from the first cubic layer and end at the last one? The situation is more complicated for the 4*H*/8*H*/4*H* QW. The sequence of cubic and hexagonal layers for 8*H* is *hccchccc*$\cdots$. It is not *a priori* clear which is the boundary layer between the 4*H* and 8*H* regions. As a matter of fact, it is unclear whether there is a sharp boundary between the two polytypes. Another important feature of the SiC polytypes is the variation of the spontaneous polarization field. For bulk materials, the polarization is strong in 2*H* and 4*H* SiC, relatively weak in 8*H*, and null in 3*C* SiC. It is interesting to examine how polarization changes when the polytypes form a QW or superlattice structure.

II. METHOD AND QW MODEL

In order to study the QW state of heteropolytype QW and address the issue of polarization, polytype boundary, and whether the 8*H* inclusion is a single well or a double well, we perform first-principles calculations for an 4*H*/8*H*/4*H* and a 4*H*/3*C*/4*H* QW model structures. The calculations are performed by means of the VIENNA *ab initio* SIMULATION PACKAGE (VASP) program.[16,17] The projector augmented wave (PAW) potentials[18,19] and the Heyd-Scuseria-Ernzerhof (HSE) hybrid functional[20,21] with 25% mixing of Hartree-Fock exchange are used in the calculations. The calculated band gaps for the bulk materials are in very good comparison with the experimental values. For example, as shown in Table I, the low temperature band gaps of 3*C*, 4*H*, and 8*H* are 2.39, 3.27, and 2.80 eV, respectively, whereas they are obtained by HSE as 2.26, 3.21, and 2.72 eV, respectively. HSE also resolves nicely the total energies of different polytypes. It agrees well with the experiments and the previous calculations on the order of polytype stability,[25–27] i.e., 4*H* is the most stable and 2*H* is significantly higher than 3*C* and 4*H*. The total energies of 6*H* and 8*H* are in between those of 3*C* and 4*H*.

Our QW calculations are performed for a supercell containing 20 bilayers of Si and C. For the 4*H*/8*H*/4*H* QW [Fig. 1], the sequence of the stacking[28] is *ABCBAB—CBACBCAB—CBABCB* or ↑↑↓↓↑↑ | ↓↓↓↓↑↑↑↑ | ↓↓↑↑↓↓, or *hchchchccchccchchchc*, where parallel spins mean cubic *c* and antiparallel spins means hexagonal *h* stackings. The size of the nominal 8*H* region is eight bilayers which is about 2 nm wide. Similarly, the sequence for the 4*H*/3*C*/4*H* QW is *ABCBABCB—ABCABC—ACBCAC* or ↑↑↓↓↑↑↓↓ | ↑↑↑↑↑↑ | ↓↓↑↑↓↓, or *hchchchcccccchchchc*. The calculation results including the layer-by-layer partial density of states (PDOS) and the wave functions of the QW states are shown in Fig. 2 for 8*H* inclusions and in Fig. 4 for 3*C* inclusions.

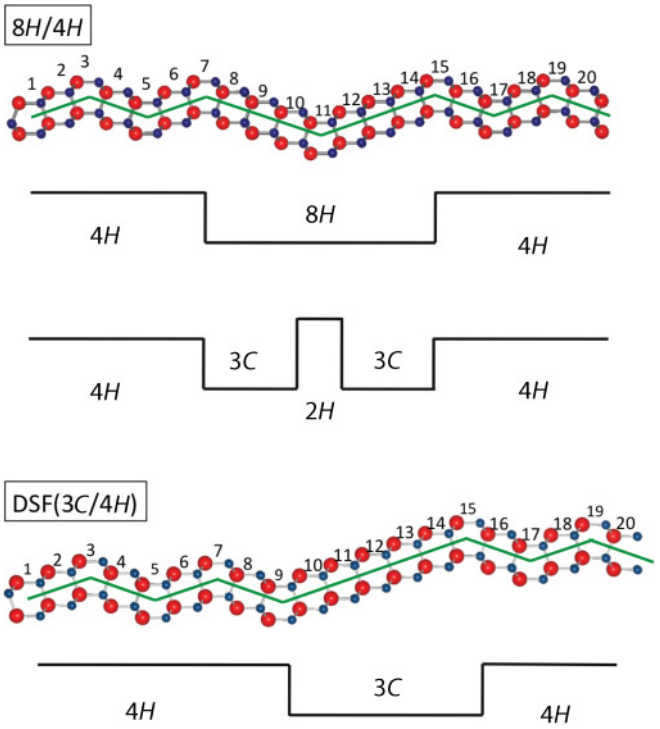

FIG. 1. (Color online) Diagram of $8H$ and $3C$ inclusions in a $4H$ SiC matrix. The single well and double well models of $8H$ inclusion in $4H$ SiC are shown. The large (red in color) and the small (blue) balls stand for the Si and the C atoms, respectively. The layers' numbers denote the Si-C bilayers consisting of Si atoms in one stack and the C atoms occupying the preceding stack.

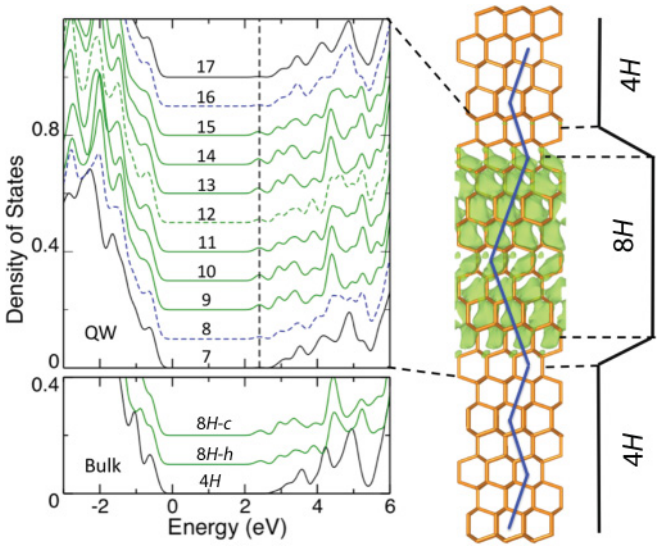

FIG. 2. (Color online) The layer-by-layer PDOS and the wave function (shown as a green isosurface in the right panel) of the QW state of an $8H$ inclusion in $4H$. The layer number is as shown in Fig. 1. For comparison, the PDOS of cubic and hexagonal layers of $8H$ and the density of states (DOS) of bulk $4H$ are also shown.

III. RESULTS

By comparing the layer PDOS of an $8H/4H$ QW with the PDOS of bulk $4H$ and $8H$ SiC, we can identify the regions of $4H$ and $8H$ in the QW. As shown in Fig. 2, the PDOS of layers 9 to 15 can be identified as $8H$ layers, whereas layers 1–7 and 17–20 are $4H$ layers. The major difference is the existence of states at the energy of about 2.4 eV. Interestingly, not only the cubic layers but also the hexagonal layer in the $8H$ region show this QW state. Indeed the PDOS of layers 9 to 15 show similar PDOS, indicating that the QW states are uniformly distributed in $8H$, a feature of a single QW structure. The wave function of the QW state as shown in Fig. 1 also indicates that the $4H/8H/4H$ behaves as a single QW. On the other hand, we do notice a reduction of the wave function amplitude and the PDOS value at the center of the $8H$ region (layer 12), indicating a strong barrier effect of the $2H$ layer at the center of $8H$ region. This layer's PDOS is different from the hexagonal layers in bulk $8H$, the PDOS of which, as shown in Fig. 2, is almost identical to the PDOS of a cubic layer, indicating the uniform distribution of the band edge wave functions throughout a given polytype. The layers 8 and 16 show a PDOS that is almost identical to $4H$. Therefore, the $8H$ region can be considered to be only 7 layers instead of 8 layers thick, and it has a quite clear boundary to $4H$ regions.

TABLE I. Structural parameters, total energies, and band gaps calculated by HSE functions. For comparison, the experimental band gaps are also listed. The total energy is relative to the energy of $4H$ per atom.

	a (Å)	c/a	E_{tot}(meV)	E_g(eV)	E_g(expt.)
$2H$	3.0748	1.634	3.3	3.219	3.30[22]
$4H$	3.0711	1.637	0.0	3.211	3.265[23]
$6H$	3.0715	1.636	0.1	2.980	3.023[24]
$8H$	3.0728	1.635	0.2	2.722	2.80[2]
$3C$	3.0741	1.633	0.7	2.263	2.39[2]

Our calculations confirm that the $4H/8H/4H$ is of type II, i.e., the electron QW states are localized in the $8H$ region whereas the hole QW states localize in the $4H$ region. The energy difference between the electron and the hole state is found to be 2.74 eV. This value is very close to the low temperature photoluminescence (PL) measurements of 2.72 (Refs. 14 and 29) and 2.672 eV (Ref. 15). In a recent study, Robert *et al.*[15] found that the recombination energy is overestimated by about 200 meV by an effective mass approach for a single QW model. They argue that a double well model that consists of two $3C$ wells separated by a single $2H$ barrier layer can reduce the recombination energy to 2.68 which is in good comparison with the experimental PL value. They thus concluded that $8H$ inclusion in $4H$ should actually be treated as a double quantum well. Our calculations do not agree with this conclusion. We think the overestimation of the recombination energy is caused by the use of the effective mass approximation, which is not applicable to this ultrathin quantum well system.

Next, we check the position of the QW level, which is the conduction band minimum (CBM) of our model system, relative to the CBM of ideal $4H$ SiC. In order to compare the absolute value of these two systems, we line up the electrostatic potential at PAW sphere of the C atom in the center of the $4H$ region in our model system and the same potential of the C

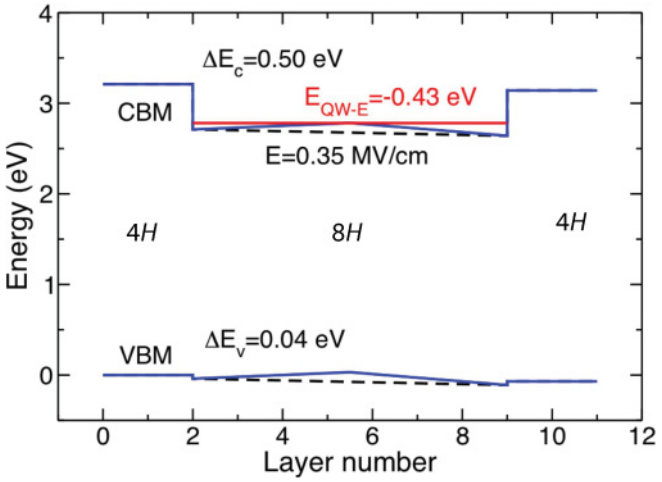

FIG. 3. (Color online) The band diagram of the $4H/8H/4H$ QW. The energies are aligned to the valence band maximum (VBM) position of bulk $4H$ SiC. The red line shows the first electronic state in the QW. The black (dashed) lines show the average spontaneous potential in the QW. The electric field inside the QW is calculated to be around 0.35 MV/cm.

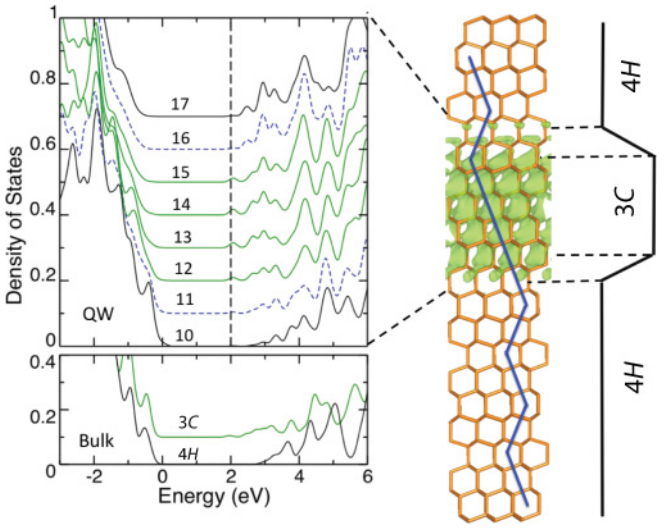

FIG. 4. (Color online) The layer-by-layer PDOS and the wave function of the QW state of a $3C$ inclusion in $4H$. The layer number is as shown in Fig. 1. For comparison, the DOS of bulk $3C$ and $4H$ are also shown.

atom in bulk $4H$. A sketch of the band diagram and the first electronic state in the $4H/8H/4H$ QW is shown in Fig. 3. It is interesting to notice that this value is larger than that of a single stacking fault (0.27 eV)[25,30] and smaller than that of a double stacking fault (0.67 eV).[31,32] We found that the QW state in the $8H$ region is 0.43 eV below the CBM of bulk $4H$, which is in good agreement with the experimental value of 0.39 eV.[12,33] This might be attributed to the smaller valence band offset (VBO) for $8H/4H$. The VBO and the conduction band offset (CBO) are obtained to be 0.04 and 0.50 eV, respectively. The CBO is about 0.2 eV smaller than those of $3C$ in $4H$ (Ref. 34) and $3C$ in $2H$.[5] The differences in the VBO are much less significant.

The $4H/3C/4H$ QW has been studied in a similar fashion, and the results are shown in Fig. 4. The region of PDOS that shows obvious $3C$ features (a peak at around 2.1 eV from the VBM) ranges from layer 12 to layer 15, which covers four layers in contrast to the five cubic layers in the double stacking fault (DSF) model. The boundary layers (11 and 16) show very small feature of $3C$ around 2.1 eV, indicating that the QW state penetrates into these layers. In addition, the location of the QW state also shows a distinct shift toward the right hand side of the QW because the cubic layers in the DSF model starts from layer 10 and extend to layer 14. The extension and the shift of the QW state can also be seen from the wave function of the QW state which is also shown in Fig. 4. As will be discussed below, the shift of the QW state is the result of a strong polarization field in the $4H/3C/4H$ QW.

The QW state is found to be at 0.68 eV below the CBM of $4H$ SiC. This value is very close to the value of 0.67 eV obtained by local density functional (LDA)[31,32] indicating that the position of the QW state can be well captured by local and semilocal functionals. The VBO and the CBO are found to be 1.01 and 0.014 eV, respectively. The $4H/3C/4H$ is also a type-II quantum well with a very shallow barrier for the holes.

At last, we study the polarization of heterojunctions formed by SiC polytypes. We plot the electrostatic potentials at the PAW spheres of all the C atoms [Figs. 5(a) and 5(b)]. The potential profiles obtained from the plane-averaged electrostatic potential show the same features and values as Fig. 5. As shown in Fig. 5, the polarization potential varies more significantly in a $4H/3C/4H$ QW than in a $4H/8H/4H$ QW. The large polarization field in a $4H/3C/4H$ QW may cause a large shift of the QW state. This effect can also be seen in a one-dimensional Schrödinger-Poisson simulation. In this simulation, the size of the QW is chosen the same as the width

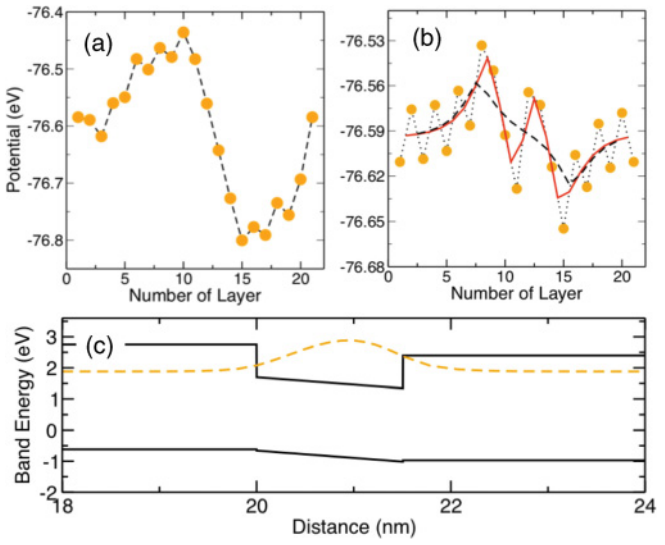

FIG. 5. (Color online) (a) The average electrostatic potential of a SiC heteropolytype QW formed by a $3C$ inclusion in $4H$. (b) The average electrostatic potentials of an $8H$ inclusion in $4H$, in which the dotted, the solid, and the dashed lines are averaged over 2, 4, and 8 layers, respectively; please note the different scale. (c) Band diagram of a $3C$ inclusion in $4H$ SiC with a simulated one-dimensional (1D) wave function.

of the DSF. The parameters, such as the CBO and VBO, are chosen from the values obtained earlier in this paper. As shown in Fig. 5(c), the center of the wave function has been shifted from the center of the QW toward the right by the polarization field. More importantly, the amplitude of the wave function at the right edge of the QW is significantly larger than that at the left side, and the wave function penetrates deeply (3–5 Å or 1–2 layers) into the $4H$ region. This explains the observed shift of the $3C$ features in the calculated PDOS.

The problem of whether a $4H/8H/4H$ QW should be considered a single or double well can also be viewed from the point of view of the polarization potential. For a single well, we expect a monotonic function; for a double well, we expect a W-shaped potential. The potential shows a zig-zag shape in the $4H$ region and a W shape in the $8H$ region [see Fig. 5(b)]. After make a running average of every four layers (solid line), the potential in $4H$ region become smooth and monotonic, whereas in the $8H$ region it retains a W shape. However, if we increase the number of layers over which we average to eight, the potentials in both $4H$ and $8H$ regions are smooth and monotonic. This slope should correspond to the difference in polarization of $8H$ and $4H$. We also note that the W-shaped barrier in potential in the $8H$ region is much smaller than the VBO and does not warrant considering the system as a double well, but rather as a single well with a little bump in the middle.

IV. CONCLUSIONS

In this paper, we studied some fundamental issues for heterojunctions formed by SiC polytypes: namely the question of how to locate the boundary between the layers, the nature of the QW localized states, and the polarization induced potentials by applying first-principles calculations. The importance of understanding these issues goes beyond SiC. Although the energy differences between different polytypes for other materials than SiC are usually much larger in comparison with those for SiC, these energy differences vary with the size of the crystallite, and therefore the polytypes and the corresponding heteropolytype structures may form at the nanoscale.[35–37]

Our calculations show that the $8H$ inclusion in a $4H$ matrix should be treated as a single quantum well rather than a double QW consisting of two thin regions of $3C$ and a hexagonal barrier layer at the center. Although both $8H$ and $3C$ inclusions show a distinctive boundary to the $4H$ regions, it may differwith the nominal boundary in the constructed model. The lowest QW state in a $4H/3C/4H$ QW shifts toward the right and penetrates into the $4H$ region due to the strong polarization field. Our calculations also yield the positions of QW states, the conducting and valence band offsets in good comparison with available experimental results. Furthermore, we found that polarization is a local property and the total potential shift over a region of nonzero polarization can be obtained by adding the contributions of single layers.

ACKNOWLEDGMENTS

The paper is partially supported by ONR. M.-S.M. thanks the ConvEne-IGERT Program under project No. NSF-DGE 0801627. The calculations were performed at the Ohio Supercomputing Center (OSC) under Project No. PDS0145 and at the high performance computing clusters run by the California NanoSystems Institute (CNSI).

[1] *Properties of Advanced Semiconductor Materials: GaN, AlN, InN, BN, SiC, SiGe*, edited by M. E. Levinshtein, S. L. Rumyantsev, and M. S. Shur (John Wiley & Sons, Inc., New York, 2001).
[2] W. J. Choyke, D. R. Hamilton, and L. Patrick, Phys. Rev. **133**, 1163 (1964).
[3] W. R. L. Lambrecht, S. Limpijumnong, S. N. Rashkeev, and B. Segall, Phys. Status Solidi B **202**, 5 (1997).
[4] F. Bechstedt and P. Käckell, Phys. Rev. Lett. **75**, 2180 (1995).
[5] M. S. Miao and W. R. L. Lambrecht, Phys. Rev. B **68**, 155320 (2003).
[6] San-huang Ke, Jian Zi, Kai-ming Zhang, and Xi-de Xie, Phys. Rev. B **54**, 8789 (1996).
[7] R. S. Okojie, M. Xhang, P. Pirouz, S. Tumakha, G. Jessen, and L. Brillson, Appl. Phys. Lett. **79**, 3056 (2001).
[8] L. J. Brillson, S. Tumakha, G. H. Jessen, R. S. Okojie, M. Zhang, and P. Pirouz, Appl. Phys. Lett. **81**, 2785 (2002).
[9] J. Q. Liu, H. J. Chung, T. Kuhr, Q. Li, and M. Skowronski, Appl. Phys. Lett. **80**, 2111 (2002).
[10] S. Bai, R. P. Devaty, W. J. Choyke, U. Kaiser, G. Wagner, and M. F. MacMillan, Appl. Phys. Lett. **83**, 3171 (2003).
[11] Y. Ding, K.-B. Park, J. P. Pelz, K. C. Palle, M. K. Mikhov, B. J. Skromme, H. Meidia, and S. Mahajan, Phys. Rev. B **69**, 041305(R) (2004).
[12] K.-B. Park, Y. Ding, J. P. Pelz, M. K. Mikhov, Y. Wang, and B. J. Skromme, Appl. Phys. Lett. **86**, 222109 (2005).
[13] H. Fujiwara, T. Kimoto, T. Tojo, and H. Matsunami, Mater. Sci. Forum **483–485**, 151 (2005).
[14] S. Izumi, H. Tsuchida, T. Tawara, I. Kamata, and K. Izumi, Mater. Sci. Forum **483–485**, 323 (2005).
[15] T. Robert, S. Juillaguet, M. Marinova, T. Chassagne, I. Tsiaoussis, N. Frangis, E. K. Polychroniadis, and J. Camassel, Mater. Sci. Forum **615–617**, 339 (2009).
[16] G. Kresse and J. Hafner, Phys. Rev. B **47**, 558 (1993).
[17] G. Kresse and J. Furthmuller, Phys. Rev. B **54**, 11169 (1996).
[18] P. E. Blochl, Phys. Rev. B **50**, 17953 (1994).
[19] G. Kresse and D. Joubert, Phys. Rev. B **59**, 1758 (1999).
[20] J. Heyd, G. E. Scuseria, and M. Ernzerhof, J. Chem. Phys. **118**, 8207 (2003).
[21] J. Heyd, G. E. Scuseria, and M. Ernzerhof, J. Chem. Phys. **124**, 219906 (2006).
[22] L. Patrick, D. R. Hamilton, and W. J. Choyke, Phys. Rev. **143**, 526 (1966).
[23] L. Patrick, W. J. Choyke, and D. R. Hamilton, Phys. Rev. A **137**, 1515 (1965).

[24]W. J. Choyke and Lyle Patrick, Phys. Rev. **127**, 1868 (1962).
[25]M. S. Miao, S. Limpijumnong, and W. R. L. Lambrecht, Appl. Phys. Lett. **79**, 4360 (2001).
[26]S. Limpijumnong and W. R. L. Lambrecht, Phys. Rev. B **57**, 12017 (1998).
[27]V. Heine, C. Cheng, and R. J. Needs, J. Am. Ceram. Soc. **74**, 2630 (1991).
[28]For a full description of the stacking notations, see, e.g., Ref. 5. Briefly, the Si and C atoms each form close packed layers; A,B,C refer to the different sites the next layer can be deposited on a closed packed layer of spheres; $\uparrow,\downarrow$ mean we go up in the alphabet in the ABC notation; and c (h) mean parallel (antiparallel) "pseudospins" $\uparrow\uparrow$ ($\uparrow\downarrow$).
[29]G. Feng, J. Suda, and T. Kimoto, Appl. Phys. Lett. **92**, 221906 (2008).
[30]H. Iwata, U. Lindefelt, S. Öberg, and P. R. Briddon, Phys. Rev. B **65**, 033203 (2001); Mater. Sci. Forum **389–393**, 529 (2002); J. Phys.: Condens. Matter **14**, 12733 (2002).
[31]U. Lindefelt, H. Iwata, S. Öberg, and P. R. Briddon, Phys. Rev. B **67**, 155204 (2003).
[32]W. R. L. Lambrecht and M. S. Miao, Phys. Rev. B **73**, 155312 (2006).
[33]K. Park, Ph.D. thesis, Ohio State University, 2006.
[34]M. S. Miao and W. R. L. Lambrecht, J. Appl. Phys. **101**, 103711 (2007).
[35]D. Spirkoska *et al.*, Phys. Rev. B **80**, 245325 (2009).
[36]I. Zardo, S. Conesa-Boj, F. Peiro, J. R. Morante, J. Arbiol, E. Uccelli, G. Abstreiter, and A. Fontcuberta i Morral, Phys. Rev. B **80**, 245324 (2009).
[37]P. Mélinon *et al.*, Nat. Mater. **6**, 479 (2007).